



Exploring the potential of *Eucalyptus citriodora* biochar against direct red 31 dye and its phytotoxicity assessment

Riti Thapar Kapoor¹ · Selvaraju Sivamani²

Received: 15 April 2021 / Revised: 19 June 2021 / Accepted: 21 June 2021 / Published online: 5 July 2021
© The Author(s), under exclusive licence to Springer-Verlag GmbH Germany, part of Springer Nature 2021

Abstract

The feasibility of using *Eucalyptus citriodora* leaves (ECL), an abundantly available agricultural waste, for adsorption of an anionic dye, direct red 31 (DR31), adsorption from hydrous solution has been examined in the present research. The batch adsorption trials were performed to analyse the effects of pH, contact time, initial dye concentration, adsorbent dose, temperature and particle size on DR31 removal from its aqueous solution on biochar of ECL. A maximum of 97% removal of DR31 dye was observed at pH and initial adsorbate concentration of 2 and 40 mg/L by the ECL biochar, respectively. Equilibrium data were examined by Langmuir and Freundlich isotherms. Langmuir isotherm appeared as the best fit model with the highest adsorption capacity of 3.2 mg/g. The kinetic results were also examined and found pseudo-second-order to be the best fit which expressed that the adsorption rate was mainly regulated by chemisorption. ECL biochar maintained > 41.56% adsorption capacity of DR31 dye even after five adsorption–desorption consecutive cycles. Phytotoxicity studies on *Vigna radiata* substantiated the non-toxic nature of the treated DR31 dye-containing water. The present study reveals that the biochar of ECL can be utilized as a cost-effective adsorbent to make the dye-contaminated wastewater reusable.

Keywords *E. citriodora* · Leaves biochar · Direct red 31 · Isotherm · Kinetics · Regeneration · Phytotoxicity

1 Introduction

The availability of pure and safe water is essential for the health of human beings, ecosystem and sustainable development. The continuous decline in groundwater table and deterioration of water quality is the matter of great concern. Dyes are vastly used to produce colour onto the substrate in textile, paint, rubber, plastics, cosmetic, pharmaceutical, food, pulp and paper industries [11, 54]. Increased demand and exploitation of dyes in different manufacturing units has led to the inadvertent release of dye-contaminated water directly into the water bodies resulting in environmental pollution and health problems [3, 22, 30, 53]. During the dyeing process, a significant amount of dye (approximately 10–15%) remains unbound, and it is mislaid in water and discharged as a coloured effluent from production units [18].

Dyes are resistant to removal by conventional methods from their aqueous media because of its high solubilizing capacity in water [15, 33]. Dyes are a despicable type of pollutant, and their presence in minute concentration (10^3 µg/L) in the effluent is obvious and undesirable [45]. The presence of colour in water poses a serious threat to the environment, affecting light penetration and thereby reducing photosynthesis and dissolved oxygen, water quality and cause toxic impacts on the aquatic ecosystem [56]. Azo dyes have $-N = N$ linkages and are widely used in textile industries because of low cost, solvable and stable nature. Azo dyes and their intermediary products show carcinogenic, toxic and mutagenic impacts on a living organism [7]. The contamination of water by dye not only adversely affects the aquatic life but may also cause entry of pollutants into the food chain harming living organisms by producing carcinogenic and mutagenic effects [55]. Hence, it is an urgent requirement to develop an economical and effective way of dealing with industrial effluent in the face of ever-expanding manufacturing activities.

Direct red 31 (DR31), miscible in water, is an anionic azo dye used mainly to colour cotton and silk fabrics. It is also used in paper and printing industries. Myriads of

✉ Riti Thapar Kapoor
rk Kapoor@amity.edu

¹ Amity Institute of Biotechnology, Amity University, Noida, India

² Salalah College of Technology, University of Technology and Applied Sciences, Salalah, Oman

physical and chemical methods such as photocatalytic degradation, osmosis membrane distillation, nanofiltration, coagulation-flocculation, ozonation and cloud point extraction have been employed for dye removal from effluent [35, 51, 59]. Above mentioned techniques are potent, but their implementation is not feasible at large scale due to prolonged operation time, excessive use of chemicals, requirement of labours, high cost and sludge generation which causes secondary pollution [29].

The adsorption is developing as an alternative method for dye removal from industrial effluent due to its simplicity of design, convenience, efficiency, ease of operation, eco-friendly, non-expensive and flexible nature [42, 46]. Biochar (carbonaceous substance generated by biomass pyrolysis under zero or limited oxygen supply) has been proved effective in enhancing carbon sequestration, waste recycling, soil management and wastewater treatment [10, 17]. In this regard, biochar has appealed significantly for removal of dyes due to their structural pores with large surface area and cost-effective production due to availability of substantial agro-waste biomass (Zazycki et al. 2018; [12]. Earlier workers have reported unconventional, economical agricultural waste materials for removal of dye and other pollutants from wastewater such as walnut shell [9], jackfruit leaf powder [44], *Sonchus* fruit plant [20], pine wood [34], *Jatropha* husk [25], bael shell [48], coffee husk [11], wood waste [26] and palm kernel shell [31].

Eucalyptus citriodora (family Myrtaceae), commonly known as lemon-scented eucalyptus, is a readily available tree widely accessible in different parts of India. *E. citriodora* leaves (ECL) exhibits antibacterial, antispasmodic, antiseptic and anti-inflammatory properties due to the presence of volatile oil [27]. Eucalyptol, essential oil present in leaves of *E. citriodora*, has been used for the treatment of bronchitis, sinusitis, asthma, etc. [14]. DR31 was taken for this study due to its wide application in industries and slow degradation ability. Unfortunately, no report is available in the literature on the use of ECL for adsorption of DR31 dye. The scientific community is now searching the potential of agro-waste-based biochar for removal of contaminants from water, owing to their huge availability, high efficiency and cost-effectiveness. Therefore, the aim of the present investigation was to explore potential of using ECL biochar for removal of anionic dye (DR31) from wastewater. The effects of pH, biochar amount, size of particles, dye concentration, temperature and exposure time were assessed together with isotherm, kinetic and thermodynamic parameters to explore the efficacy of biochar prepared from ECL for removal of DR31. Also, adsorbent regeneration and phytotoxicity studies were carried out. Surface morphology and functional groups characterisation were performed using SEM and FTIR, respectively.

2 Materials and methods

2.1 Biochar preparation from *E. citriodora* leaves and proximate analysis

The leaves of *E. citriodora* were collected from surrounding areas of Amity University campus, Noida. The leaves were washed with tap water for 5 min, then twice with double distilled water to remove dirt and dried in the shade for 4 days to reduce moisture content. A stainless-steel pyrolysis reactor was utilized for biochar production with the gaseous nitrogen provided for the non-reactive environment inside pyrolyser. An electric heater was used to regulate the temperature. Dried leaves were crushed, and 2.5 kg of the leaves were pyrolysed at 500 °C for 3 h. The ECL biochar was cleaned with warm Milli-Q water and subsequently dried at 75 °C for 2 h in an oven to inhibit the presence of microbes for further batch adsorption experimental runs (Talha et al. 2018). The proximate analysis of biochar prepared from ECL was done to examine its stability towards the thermochemical conversion process. The proximate analysis was performed to estimate the moisture content, volatile matter, ash and fixed carbon contents.

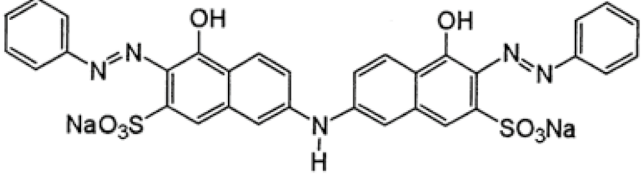
2.2 Dye stock solution preparation

DR31 dye, also known as DR12B, was procured from Sigma-Aldrich. DR31 has 2 azo, di-sulfonic acid groups and an amine group. The diazenyl group is responsible for covalent bonds formation between dye and adsorbent. A stock solution of DR31 dye (200 ppm) was made initially with distilled water, and it was diluted appropriately to produce required concentrations. The dye absorbance was calculated by using UV–vis spectrophotometer by scanning from 400 to 700 nm, and absorbance maximum (λ_{\max}) for DR31 dye was observed at 520 nm (Table 1).

2.3 Batch adsorption experiments

Batch experiments were conducted to explore the relevancy of ECL biochar (ECLB) as an adsorbent for DR31 dye removal. The various variables such as the effects of pH (2–10), adsorbent amount (0.2–1.0 g), particle size (0–500 μm), dye concentration (20–100 ppm), temperature (298.15–323.15 K) and exposure time (0–50 min) were studied at a constant agitation speed of 120 rpm for DR31 dye removal from aqueous solution on produced biochar of ECL. The experiments were conducted by pouring 100 mL of DR31 dye solution (20, 40, 60, 80 and 100 ppm) in five different Erlenmeyer flasks with five varied biochar amount (0.2, 0.4, 0.6, 0.8, 1.0 g) prepared from ECL. The samples

Table 1 Properties of DR31 dye

Dyestuff	DR31
C.I. Number	C.I.29100
Appearance	Red-brown coloured powder
IUPAC Name	2-Naphthalenesulfonicacid,7,7'-iminobis[4hydroxy-3-(2-phenyldiazenyl)-],sodium salt (1:2)
Empirical Formula	C ₃₂ H ₂₁ N ₅ Na ₂ O ₈ S ₂
Molecular Weight	713.7 g/mol
Molecular Structure	
λ _{max}	520 nm

were taken out at regular interval from incubator shaker, and analysis was done by standard procedure. A UV–vis spectrophotometer ($\lambda_{\max} = 520$ nm) was used to determine dye concentration before and after treatment. Removal efficiency at each interval was calculated by the given formula:

$$\text{Percentage removal of DR31 dye} = \frac{(C_0 - C_t)}{C_0} \times 100$$

where C_0 and C_t are initial and final concentrations of DR31 dye in mg/L in sample, respectively.

2.4 Adsorption isotherms

The isotherm models were used to interpret sorption equilibrium. One hundred millilitres of DR31 dye (20–100 mg/L) solution was mixed with 5 different initial concentrations of DR31. The equilibrium solution concentrations and adsorption capacity were evaluated with the suitability of the isotherm.

2.4.1 Langmuir isotherm

The Langmuir isotherm model speculates that the adsorption process takes place in a monolayer mode. It also explains that, at a constant temperature, adsorption energy is constant over the adsorbates' layer on the adsorbents' surface [6]. Langmuir equation is expressed as follows:

$$\frac{C_e}{q_e} = \frac{1}{q_m K_L} + \frac{C_e}{q_m}$$

where q_e (mg/g) is the dye amount adsorbed at equilibrium, q_m (mg/g) is the maximum dye amount adsorbed, C_e

is the concentration of dye at equilibrium (mg/L) and K_L is Langmuir constant associated with the bonding strength of adsorbate on the adsorbent.

2.4.2 Freundlich isotherm

Freundlich isotherm elucidates adsorbate molecules' distribution between feed solution and adsorbent at equilibrium. The isotherm assumes an exponential disparity in surface energy of active sites during adsorption and logarithmic decrease in the heat of adsorption [41]. The Freundlich equation can be written as follows:

$$\ln q_e = \ln K_F + \left(\frac{1}{n}\right) \ln C_e$$

where Freundlich constants such as n and K_F are the intensity of adsorption and adsorption capacity, respectively. The value of n indicates nature of process, $n < 1$ signifies chemisorption, $n > 1$ implies physisorption and $n = 1$ denotes linear adsorption.

2.5 Adsorption kinetics

Adsorption kinetic investigations permit researchers to determine equilibrium time and adsorption rate through adsorption modelling. Pseudo-first and second-order kinetic models were utilized for estimation of rate constants in the adsorption process.

Pseudo-first-order kinetic mechanism can be represented as follows [32]:

$$\ln(q_e - q_t) = \ln q_e - k_1 t$$

where q_e and q_t are amount of DR31 dye adsorbed at equilibrium and time t , and k_1 is rate constant of pseudo-first-order adsorption (min^{-1}).

Pseudo-second-order reaction can be analysed by the following equation [21]:

$$\frac{t}{q_t} = \frac{1}{k_2 q_e} + \frac{t}{q_e}$$

where q_e is the quantity of DR31 dye adsorbed on biochar at equilibrium and k_2 is pseudo-second-order adsorption rate constant ($\text{g/mg}\cdot\text{min}$).

2.6 Thermodynamic analysis

The free energy, enthalpy and entropy changes were analysed for adsorption of DR31 dye onto ECL biochar. The thermodynamic parameters were evaluated using the following equations:

$$\Delta G^0 = -RT \ln K_d$$

$$K_d = \frac{q_e}{C_e}$$

$$\Delta G^0 = \Delta H^0 - T \Delta S^0$$

After rearranging the equation, changes in free energy, enthalpy and entropy were evaluated by using the curve fitting method for the adsorption process.

2.7 Regeneration analysis

In the regeneration analysis, 100 mL of DR31 dye solution of various concentrations (20–100 mg/L) was mixed with the used adsorbent (ECL biochar), and the resulting solution was placed under shaking incubator (180 rpm) at 32 °C for 45 min. The dye-loaded biochar was separated by centrifugation, and DR31 dye residue in the supernatant was analysed to know the amount of dye adsorbed by biochar particles. After that, 0.1 g dye-loaded dried biochar (dried at 50 °C for 7–8 h) was mixed to the desorbing solution (1 N each of HCl and NaOH) and shaken at 180 rpm for 45 min. DR31 dye released in desorbing solution was determined by UV–visible spectrophotometer. The adsorbent (biochar) separated from the desorbing solution was cleaned with the distilled water 3–4 times to detach the desorbing solution. The washed biochar particles were dried at 50 °C up to 8–10 h for further use. The regeneration test was repeated five cycles for exploring the recyclability of the utilized biochar. The desorption (%) of dye was measured by the given formula:

$$\text{Percentage desorption} = \frac{\text{Amount of dye desorbed}}{\text{Amount of dye adsorbed}} \times 100$$

2.8 Phytotoxicity assay

The toxicity of DR31 dye before and after treatment with ECL biochar was examined on *Vigna radiata* seeds. *V. radiata* seeds were cleaned with tap water, sterilized the surface using the diluted solution of NaOCl (10% (w/v)) for 5–7 min for microbial disinfection and further washed for 4–5 times with double distilled water. Two treatment sets were prepared in which mung bean seeds were soaked in (i) DR31 dye solution (40 mg/L) and (ii) ECL biochar treated dye solution for 4 h, respectively. After 4 h, mung bean seeds were transferred into sterilized Petri dishes (20 cm diameter) and kept in a seed germinator for 1 week under 85% relative humidity at 25 ± 2 °C with a photoperiod of ½ day [23]. The germination of seed and other growth parameters such as seedling length and vigour index were assessed in control and treatment. The plumule and radicle length of seedlings were assessed after 8 days of seed sowing with a measuring scale [23]. Germination % and vigour index were calculated by the following equations (Abdul—Baki and Anderson 1973):

$$\text{Percentage germination} = \frac{\text{Total number of seeds germinated}}{\text{total number of seeds sowed}} \times 100$$

2.9 Characterisation of adsorbent

The functional groups present on ECL biochar before and after DR31 dye adsorption were analysed by using Fourier transform infrared (FTIR) spectroscopy in wavenumber ranging of 400–4000 cm^{-1} using KBr pellet technique. The external surfaces of ECL biochar before and after DR31 dye adsorption were visualized by using scanning electron microscopy (SEM) at a magnification of $\times 1000$.

2.10 Statistical analysis

Treatments were organized with three replicates in randomized block design. The data were determined by using ANOVA and SPSS software. Mean of treatment was assessed by Duncan's multiple range test at $P < 0.05$.

$$\text{Vigour index} = \text{Total seedling length in mm} \times \text{Percentage germination}$$

Table 2 Proximate analysis of ECL biochar

S. no	ECL	Weight (%)
1	Moisture content	10.71
2	Volatile matter	12.02
3	Ash content	9.78
4	Fixed carbon	67.49

3 Results and discussion

Proximate analysis of biochar prepared from *E. citriodora*.

Proximate analysis was conducted to determine the percentage of fixed carbon, volatile matter, moisture and ash contents in an ECL biochar. The data exhibited

that adsorbent has 67.49% fixed carbon, 12.02% volatile matter, 10.71% moisture and 9.78% ash contents (Table 2).

3.1 Investigations on effect of process parameters on DR31 dye adsorption by ECL biochar

3.1.1 Initial solution pH

The pH of solution plays a vital role in the dye adsorption process. The pH effect on DR31 dye removal from the aqueous solution (20–100 mg/L dye concentration) was analysed by changing pH from 2 to 10 at 27 ± 2 °C. The pH of adsorbate solution is an essential parameter for adsorption studies and considered as one of the most

Fig. 1 Effect of **a** pH, **b** time, **c** initial dye concentration, **d** adsorbent dosage, **e** temperature and **f** particle size on DR31 removal by ECL biochar

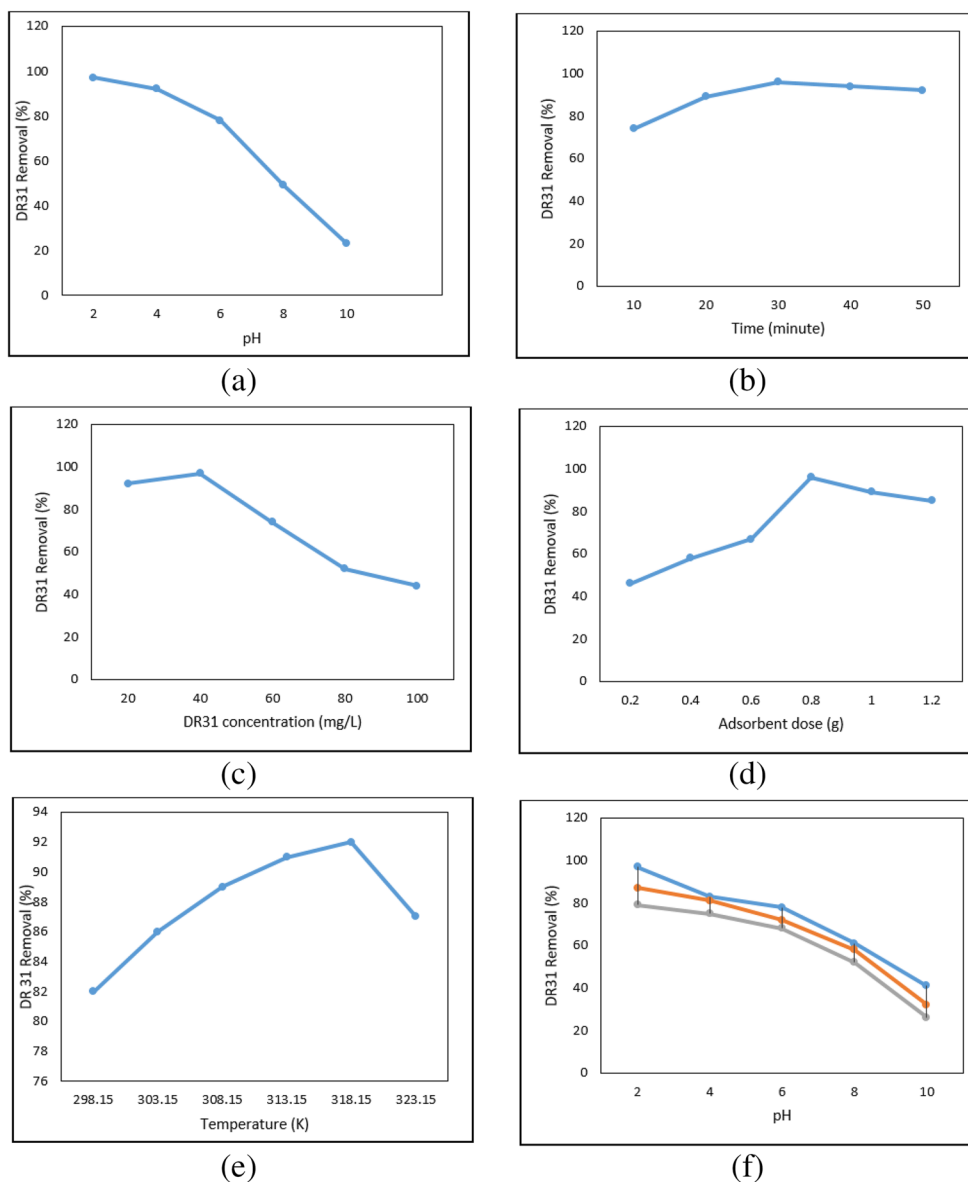


Table 3 Isotherm constants for DR31 dye adsorption by ECL biochar

Isotherm	Equation	Parameters	Value
Langmuir	$\frac{C_e}{q_e} = \frac{1}{q_m K_L} + \frac{C_e}{q_m}$	q_m (mg/g)	3.2
		K_L (l/mg)	0.0338
		R^2	0.9918
Freundlich	$\ln q_e = \ln K_F + \left(\frac{1}{n}\right) \ln C_e$	$1/n$	5.2548
		K_F (mg/g)	2.130379
		R^2	0.9424

influencing factors [24]. The maximum 97% removal of DR31 dye (40 mg/L) was observed by ECL biochar at lower pH (2) whereas 78, 49 and 23% DR31 removal was reported at pH 6, 8 and 10, respectively (Fig. 1a). DR31 dye removal was found significantly at low pH due to the participation of more H^+ in solution. At low pH, the adsorbent surface was positively charged, which attracts DR31 dye (anionic dye). Thus, the electrostatic attraction was responsible for the high rate of dye adsorption by ECL biochar at low pH.

3.1.2 Exposure time

Dye removal percentage was observed to augment with increasing contact time. Variation in dye percentage removal with contact time is shown in Fig. 1b. At earlier stages, DR31 dye removal or dye amount adsorbed was significant as compared to the end of the process. The effect of contact time on DR31 dye adsorption was studied to determine equilibrium time. DR31 dye removal 74, 89 and 96% was observed after 10, 20 and 30 min for 40 mg/L dye concentration. In the present study, 30 min was considered as equilibrium time for adsorption process because after this duration, no rise

in dye adsorption was observed. Rapid uptake of DR31 dye and attaining equilibrium in less duration indicates dye removal efficiency of biochar. The fast dye removal rate was found during an earlier stage of adsorption due to free sites availability on biochar [19]. Similar findings were observed for Azure dye adsorption on dried sunflower seed hull [43].

3.1.3 Initial DR31 dye concentration

The initial dye concentration provides energy to control mass transfer resistances of molecules between solid and aqueous phases [47]. Figure 1c shows removal of DR31 dye by ECL biochar under various dye concentrations. The dye adsorption reduces with the rise in DR31 dye concentration. With low concentration of dye, more colour removal was observed, but at high concentration of DR31, the dye removal rate was reduced due to impregnation of adsorbent surface.

3.1.4 Adsorbent dose

Adsorbent (ECL biochar) amount on DR31 dye removal was examined by varying amount from 0.2–1.2 g at different dye concentrations. DR31 dye removal was enhanced from 46 to 85% as the adsorbent dose increased from 0.2–1.2 g, observed in Fig. 1d. The maximum 96% DR31 dye removal was observed with 0.8 g of ECL biochar. The specific surface area, pore structure, particle size and functional groups present on biochar are main physico-chemical parameters that regulate dye adsorption. The rise in dye removal rate with high biochar amount may be because of increase in available active sites due to enhanced surface area and functional groups available for adsorption, thus making easier attachment of dye onto adsorption sites [4]

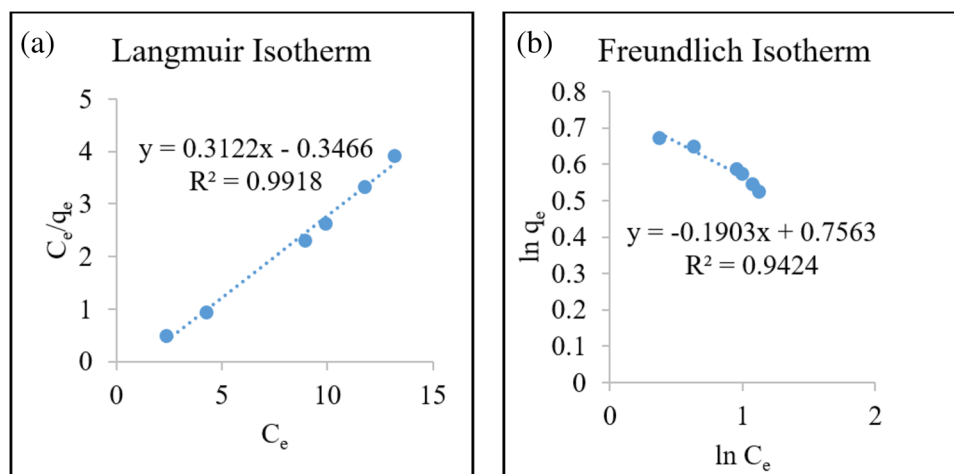
Fig 2 a Langmuir and b Freundlich isotherms for adsorption of DR31 dye by ECL biochar.

Table 4 Kinetic parameters for adsorption of DR31 dye onto *E. citriodora* adsorbent

Model	Equation	Parameters	Value
Pseudo-first-order	$\ln(q_e - q_t) = \ln q_e - k_1 t$ (min^{-1})	k_1 (min^{-1})	0.018
		q_e (mg/g)	1.893
		R^2	0.3524
Pseudo-second-order	$\frac{t}{q_t} = \frac{1}{k_2 q_e} + \frac{t}{q_e}$	K_2 (g/mg min)	0.194
		q_e (mg/g)	3.736
		R^2	0.9678

3.1.5 Temperature

DR31 dye adsorption on ECL biochar was investigated at different temperatures such as 298.15, 303.15, 308.15, 313.15, 318.15 and 323.15 K. In the present study, DR31 dye showed 82 and 86% adsorption at 298.15 and 303.15 K, respectively, and dye adsorption was enhanced to 92% at 318.15 K (Fig. 1e). The increased adsorption at high temperature was suggested to be due to rise in surface sites availability and high adsorbent porosity and pore volume.

3.1.6 Particle size

The surface area of prepared biochar is directly proportional to the removal of DR31 dye. The adsorption of DR31 dye was analysed with three different particle sizes of ECL biochar, i.e. 0–170, 230–300 and 320–500 μm . It was found that as the size of particle decreases, dye molecules adsorption enhances, might be due to availability of more surface area on small-sized particles. The diffusion resistance to mass transport is high for large-sized particles, and the internal surface of the particle may not be used for adsorption, and due to this, only a few amount of dye was adsorbed. The

impact of variation in the particle sizes on the dye adsorption rate is given in Fig. 1f.

3.2 Adsorption isotherms

Adsorption isotherm reflected how dye molecules were dispersed between liquid and solid phases at a constant temperature under equilibrium. The isotherm models provide valuable information on adsorption mechanism, surface property and adsorbent capacity. Hence, isotherm data of DR31 dye adsorption on ECL biochar was assessed by using Langmuir and Freundlich models (Table 3; Fig. 2a and b).

In the present study, Langmuir isotherm reflected better fitting model than Freundlich as observed by high correlation coefficient ($R^2 = 0.9918$). It showed monolayer coverage of DR31 dye on ECLB adsorbent [56, 57]. After calculation by the equation, Langmuir constants showed the following values: $q_m = 3.20$ mg/g and $k = 0.0338$ mg^{-1} and Freundlich constants were $K_f = 2.130379$ and $n = 5.2548$ and $R^2 = 0.9424$.

3.3 Adsorption kinetics

The kinetic study provides knowledge regarding adsorption efficiency and reaction pathway. Kinetic models were utilized to determine the adsorption of DR31 dye by ECL biochar. The coefficients of determination (R^2) were 0.3524 and 0.9678 for pseudo-first and second-order model, respectively. Pseudo-second-order kinetic model was followed due to its more correlation coefficient value (Table 4; Fig. 3a and b).

Data reflected that the adsorption process was controlled by sorption between molecules of dye and ECL biochar surface. Pseudo-second-order model was obtained in earlier reports such as adsorption of direct

Fig. 3 a Pseudo-first-order and b pseudo-second-order models or DR31 dye adsorption by ECL biochar.

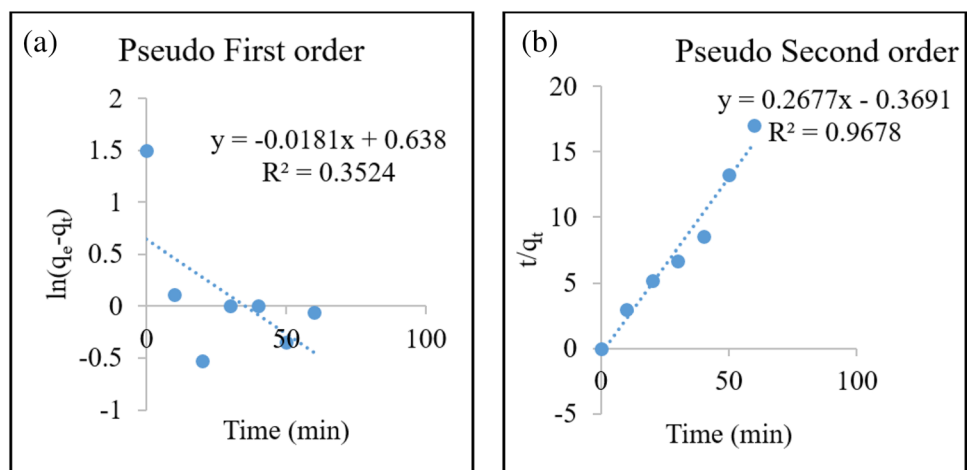


Table 5 Thermodynamic variables for adsorption of DR31 dye by ECL biochar

S. no	Temperature (K)	Free energy change (ΔG°) kJ/mol	ΔH° (kJ mol^{-1})	ΔS° (J/K)
1	298.15	-3393.07	-19.905	57.672
2	303.18	-2432.8		
3	308.15	-443.99		
4	313.15	-2418.35		
5	318.15	-2024.18		
6	323.15	-1224.85		

red 12B on garlic peel [5], adsorption of direct red 81 by *Argemone mexicana*, adsorption of crystal violet dye by *Tectona grandis* [37] and coffee husk [11].

3.4 Thermodynamic analysis

Gibb's free energy of adsorption (ΔG°), enthalpy (ΔH°) and entropy (ΔS°) changes were determined to anticipate the adsorption phenomenon. In this study, adsorption experiments were done at various absolute temperatures like 298.15, 303.15, 308.15, 313.15, 318.15 and 323.15 K (Table 5). A negative value of ΔG° at varied temperature exhibited spontaneous nature of DR31 dye adsorption onto ECL biochar [25].

The negative value of ΔH° ($-19.905 \text{ kJ mol}^{-1}$) further established that process was exothermic. The positive value of ΔS° (57.672 J/K) reflected the rise in adsorbate concentration in the solid phase. Enhanced randomness

at the solid–liquid interface was also reported during adsorption. According to Kołodyńska et al. (2017), physical adsorption carried out by electrostatic interactions. Based on the findings, DR31 dye adsorption onto ECL biochar was an exothermic and spontaneous process which was persistent with results reported in isotherm study.

3.5 Characterisation of adsorbent

Figure 4 shows the FTIR spectra of ECL biochar before and after adsorption. The functional groups present in biochar corresponds to the wavenumbers of 3700, 2275, 1600, 1450, 1150 and 1000 cm^{-1} , characteristic of the C = C, C = O and C–O bonds. In ECL biochar before adsorption, there was more change in absorbance from 1600 to 1675 cm^{-1} concerning the stretching movement of the C = C bonds of molecules in the aromatic compounds and the carboxyl group (C = O). After adsorption, the vibrational movement of C = O in the molecule was observed, which exhibits the ketone group (2275 cm^{-1}). The significant changes were noticed between 1000 and 1450 cm^{-1} attributed to the C–H and C–O bonds, indicating the ester and alcohol groups formation. In grass and wood biochar, vibrational elongation of the C = C bond was observed (Keiluweit et al. (2010)).

Figure 5 shows the scanning electron micrographs of adsorbent before and after adsorption. Figure 5a shows the adsorbent with more number of pores, which indicates that the adsorbent is prepared to adsorb adsorbate molecules. Figure b illustrates the pores covered with adsorbate molecules.

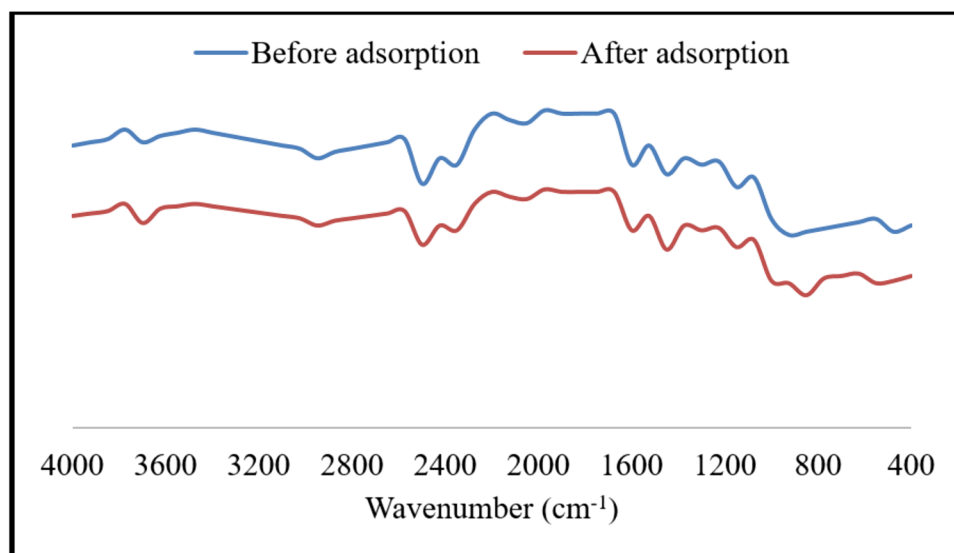
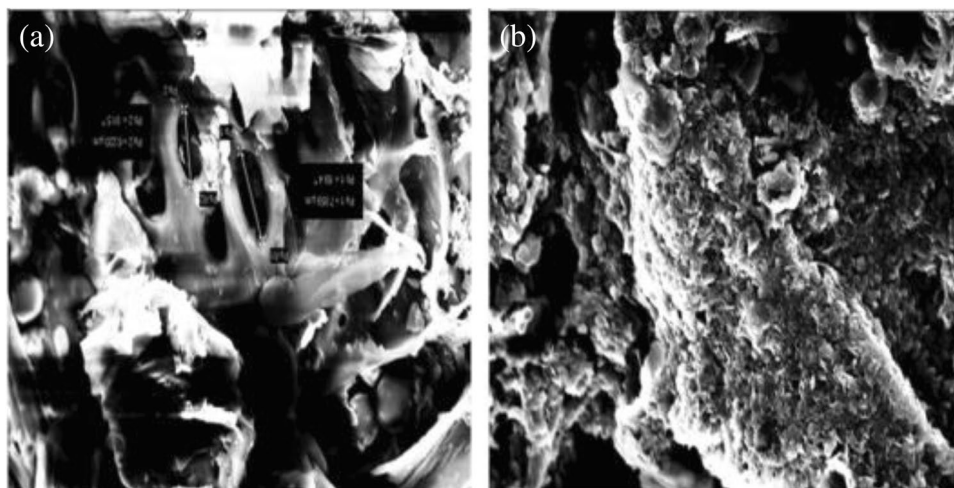
Fig. 4 FTIR of adsorbent before and after adsorption

Fig. 5 Scanning electron micrographs of ECL biochar **a** before and **b** after adsorption



3.6 Regeneration analysis

The recyclability of adsorbent is an essential index for evaluating the potential application of an adsorbent. It reduces the total cost of adsorption process and also checks secondary pollution, which may cause if these are dumped directly into the environment. The regenerated biochar showed 78.32, 66.41, 57.24, 49.63 and 41.56% DR31 dye adsorption efficiency from first to fifth cycle, respectively (Fig. 6) The reproduced biochar (ECLB) can be reapplied efficiently for DR31 dye adsorption.

3.7 Phytotoxicity assay

The ecotoxicological test, such as phytotoxicity of untreated and treated DR31 dye solution, was evaluated by observing germination and growth parameters of *V. radiata* seeds. The notable changes were reported among treatment for the following parameters such as seed germination, radicle and plumule length and vigour index of mung bean seeds. The seed germination was 98% in control, whereas DR31 dye (40 mg/L) treated *V. radiata* seeds showed only 16% germination. The mung bean seeds germination was enhanced to 83% in dye solution treated

Fig. 6 Removal of DR31 dye by ECL biochar up to five cycles

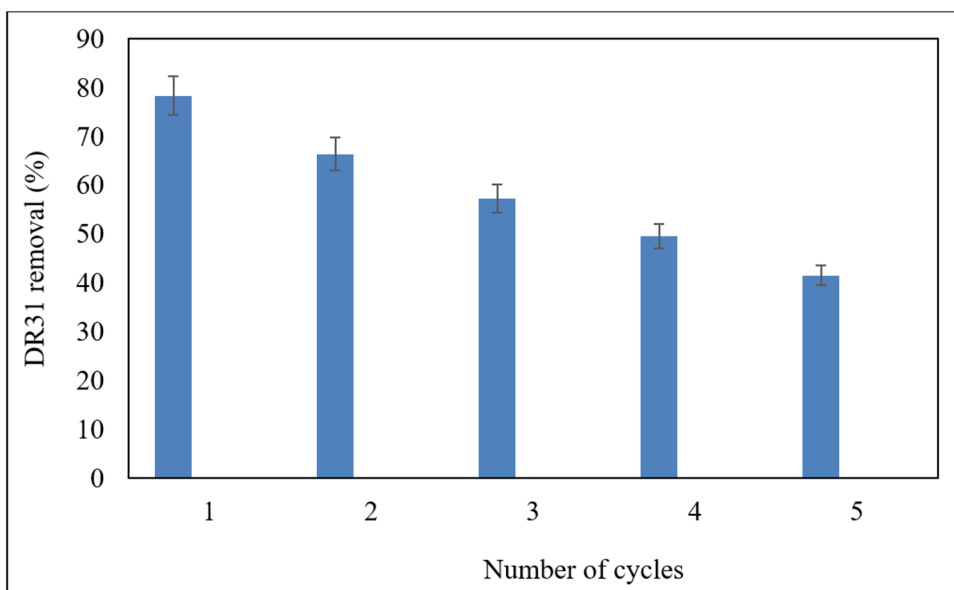


Table 6 Comparison of phytotoxicity of DR31 dye solution before and after treatment on seed germination and growth parameters of *V. radiata*

Treatment	Seed germination (%)	Plumule length (cm)	Radicle length (cm)	Vigour index
Control	98 ± 0.71	10.6 ± 0.88	3.3 ± 0.85	13,622
DR31 dye solution (40 mg/L)	16 ± 1.22	1.8 ± 0.25	0.21 ± 0.01	321.6
ECL biochar treated DR31 dye solution	83 ± 1.41	7.5 ± 0.07	2.2 ± 0.21	8439

with ECL biochar. In control, radicle and plumule length were 3.3 and 10.6 cm but decreased to 1.8 and 0.21 cm in the DR31 dye solution. ECL biochar treated dye solution reflected a significant rise in seedling length and vigour index as compared to the DR31 dye solution. The vigour index of *V. radiata* seeds exhibited the following order: control > ECL biochar treated DR31 dye solution > DR31 dye solution (Table 6).

3.8 Statistical analysis

All the experiments were carried out in triplicate, and the coefficient of variance was found within ± 10%.

3.9 Performance of the prepared ECL biochar

Efficiency of prepared ECL biochar for DR31 dye adsorption compared with other relevant studies is given in Table 7. Adsorption capacity (q_{\max}) was used for comparison. The q_{\max} value is in agreement with earlier reports, suggesting that DR31 dye can be smoothly adsorbed on ECLB. It shows ECL can be an effective and promising adsorbent for anionic dyes.

The treatment of azo dyes in wastewater is a challenging task because these dyes are electron-deficient xenobiotic complexes which are resistant to degradation. The present study revealed that ECLB is a reliable, simple, adaptable and affordable adsorbent for removal of DR31 dye from contaminated wastewater and can be used successfully at large scale.

4 Conclusion

The possibility of biochar prepared from ECL for removing DR31 was investigated in this study. FTIR spectra indicated that prepared biochar carries different functional groups which can be used for adsorption of DR31 dye. Langmuir adsorption isotherm was reported the best fit to experimental data and showed a maximum adsorption capacity of 3.20 mg/g. A negative value of ΔH° confirmed that adsorption was spontaneous and exothermic. Regenerated biochar indicated favourable results up to five consecutive cycles for DR31 dye removal. The regeneration characteristic also reflects its potential for practical application. Therefore, biochar from agro-waste, i.e. ECL, can be cost-effective adsorbent for removal of DR31 dye from industrial wastewater.

Table 7 Maximum adsorption capacity (q_{\max}) of DR31 dye with different adsorbents

Dye	Source of biochar	q_{\max} (mg/g)	Reference
DR31	Rice bran	1.23	Sankar et al. [50]
	Biogas residual slurry	3.46	Namasivayam and Yamuna [40]
	Fe (III)/Cr (III) hydroxide	5	Namasivayam and Sumithra [39]
	Banana pith	5.92	Namasivayam et al. [38]
	Hazelnut shell	18.24	Fathi and Asfaram [16]
	Biosilica/calcium alginate composite	33.78	Soltani et al. [52]
	Garlic peel	37.96	Asfaram et al. [5]
	ZnCl ₂ activated <i>Jatropha</i> husk	39	Karthick et al. [25]
	Modified magnetic ferrite nanoparticle	55.56	Mahmoodi [36]
	Rice husk	57.88	Yusra and Nawaz (2011)
	Cone shell of Calabrian pine	66.02	Deniz [13]
	ECL	3.2	This study

Acknowledgements RTK is thankful to Amity Institute of Biotechnology, Amity University, Noida for offering laboratory facilities to carry out this study.

Declarations

Competing interests The authors declare no competing interests.

References

- Abdul Baki AA, Anderson JD (1973) Viability and leaching of sugars from germinating seeds by textile, leather and distillery industries. *Ind J Environ Protec* 11:592–594
- Abu Talha M, Goswami M, Giri BS, Sharma A, Rai BN, Singh RS (2018) Bioremediation of congo red dye in immobilized batch and continuous packed bed bioreactor by *Brevibacillus parabravis* using coconut shell bio-char. *Bioresour Technol* 252:37–43. <https://doi.org/10.1016/j.biortech.2017.12.081>
- Amin MT, Alazba AA, Shafiq M (2021) Successful application of *Eucalyptus camdulensis* biochar in the batch adsorption of crystal violet and methylene blue dyes from aqueous solution. *Sustainability* 13:3600. <https://doi.org/10.3390/su13073600>
- Anbia M, Salehi S (2012) Removal of acid dyes from aqueous media by adsorption onto amino-functionalized nanoporous silica SBA-3. *Dyes Pigm.* 94(1):1–9. <https://doi.org/10.1016/j.dyepig.2011.10.016>
- Asfaram A, Fathi MR, Khodadoust S, Naraki M (2014) Removal of direct red 12B by garlic peel as a cheap adsorbent: kinetics, thermodynamic and equilibrium isotherms study of removal. *Spectrochim Acta A* 127:415–421. <https://doi.org/10.1016/j.saa.2014.02.092>
- Bharathi KS, Ramesh SPT (2013) Fixed-bed column studies on biosorption of crystal violet from aqueous solution by *Citrullus lanatus* rind and *Cyperus rotundus*. *Appl Water Sci* 3:673–687. <https://doi.org/10.1007/s13201-013-0103-4>
- Bruschweiler BJ, Merlot C (2017) Azo dyes in clothing textiles can be cleaved into a series of mutagenic aromatic amines which are not regulated yet. *Regul Toxicol Pharmacol* 88:214–226. <https://doi.org/10.1016/j.yrtph.2017.06.012>
- Callegari A, Boguniewicz-Zablocka J, Capodaglio A (2017) Experimental application of an advanced separation process for NOM removal from surface drinking water supply. *Separations* 4(4):32. <https://doi.org/10.3390/separations4040032>
- Cao J, Lin J, Fang F, Zhang M, Hu Z (2014) A new adsorbent by modifying walnut shell for the removal of anionic dye: kinetic and thermodynamic studies. *Bioresour Technol.* 163:199–205. <https://doi.org/10.1016/j.biortech.2014.04.046>
- Cao L, Yu IKM, Chen SS, Tsang DCW, Wang L, Xiong X, Zhang S, Ok YS, Kwon EE, Song H, Poon CS (2018) Production of 5-hydroxymethylfurfural from starch-rich food waste catalyzed by sulfonated biochar. *Bioresour Technol* 252:76–82. <https://doi.org/10.1016/j.biortech.2017.12.098>
- Cheruiyot GK, Wanyonyi WC, Kiplimo JJ, Maina EN (2019) Adsorption of toxic crystal violet dye using coffee husks: equilibrium, kinetics and thermodynamics study. *Scientific African* 5(e00116):1–11. <https://doi.org/10.1016/j.sciaf.2019.e00116>
- Choudhary M, Kumar R, Neogi S (2020) Activated biochar derived from *Opuntia ficus-indica* for the efficient adsorption of malachite green dye, Cu^{+2} and Ni^{+2} from water. *J Hazardous Materials* 392:122441. <https://doi.org/10.1016/j.jhazmat.2020.122441>
- Deniz F (2014) Optimization of biosorptive removal of dye from aqueous system by cone shell of Calabrian pine. *The Scientific World J.* 1–10. <https://doi.org/10.1155/2014/138986>
- Dogan H, Tasman F, Cehreli ZC (2001) Effect of gutta-percha solvents at different temperatures on the calcium, phosphorus and magnesium levels of human root dentin. *J Oral Rehab* 28:792–796. <https://doi.org/10.1046/j.1365-2842.2001.00714.x>
- Dong H, Guo T, Zhang W, Ying H, Wang P, Wang Y, Chen Y (2019) Biochemical characterization of a novel azoreductase from *Streptomyces* sp.: application in eco-friendly decolorization of azo dye wastewater. *Int J Biol Macromolecules* 140:1037–1046. <https://doi.org/10.1016/j.ijbiomac.2019.08.196>
- Fathi MR, Asfaram (2011) Investigation of kinetics and equilibrium isotherms of direct red 12B dye adsorption on hazelnut shells. *J Chem Health Risks* 1(2): 1–12
- Ferraro G, Pecori G, Rosi L, Bettucci L, Fratini E, Casini D, Rizzo AM, Chiaramonti D (2021) Biochar from lab-scale pyrolysis: influence of feedstock and operational temperature. *Biomass Conv. Bioref.* <https://doi.org/10.1007/s13399-021-01303-5>
- Forgacs E, Cserhati T, Oros G (2004) Removal of synthetic dyes from wastewaters: a review. *Environ Int* 30:953–971. <https://doi.org/10.1016/j.envint.2004.02.001>
- Gao J, Kong D, Wang Y, Wu J, Sun S, Xu P (2013) Production of mesoporous activated carbon from tea fruit peel residues and its evaluation of methylene blue removal from aqueous solutions. *Bio Resour* 8:2145–2160
- Heravi MM, Abasion Z, Morsali A, Ardalan P, Ardalan T (2015) Biosorption of direct red 81 dye from aqueous solution on prepared sonchus fruit plant, as a low cost biosorbent: thermodynamic and kinetic study. *J Appl Chem* 9:17–22
- Ho YS, Mckay G (1999) Pseudo-second-order model for sorption processes. *Process Biochem* 34(5):451–465. [https://doi.org/10.1016/S0032-9592\(98\)00112-5](https://doi.org/10.1016/S0032-9592(98)00112-5)
- Hou Y, Zhang R, Yu Z, Huang L, Liu Y and Zhou Z (2017) Accelerated azo dye degradation and concurrent hydrogen production in the single-chamber photocatalytic microbial electrolysis cell. *Bioresour Technol.* 224 (Supplement C): 63–68. <https://doi.org/10.1016/j.biortech.2016.10.069>
- ISTA (2008) International rules for seed testing. International Seed Testing Association. ISTA Secretariat, Switzerland
- Kapur M, Mondal MK (2013) Mass transfer and related phenomena for Cr(VI) adsorption from aqueous solutions on *Mangifera indica* sawdust. *Chem. Eng. J.* 218:138–146. <https://doi.org/10.1016/j.cej.2012.12.054>
- Karthick K, Namasivayam C, Pragasam LA (2017) Removal of direct red 12B from aqueous medium by ZnCl_2 activated Jatropa husk carbon: adsorption dynamics and equilibrium studies. *Ind J Chem Technol* 24:73–81
- Kelm MAP, da Silva Júnior MJ, de Barros Holanda SH, de Araujo CMB, de Assis Filho R B, Freitas EJ, dos Santos DR, da Motta Sobrinho MA (2019) Removal of azo dye from water via adsorption on biochar produced by the gasification of wood wastes. *Environ Sci Pollut Res.* <https://doi.org/10.1007/s11356-018-3833-x>
- Kharwar RN, Gond SK, Kumar A, Mishra A (2010) A comparative study of endophytic and epiphytic fungal association with leaf of *E. citriodora* Hook., and their antimicrobial activity. *World J Microbiol Biotechnol.* 26:1941–1948. <https://doi.org/10.1007/s11274-010-0374-y>
- Kolodynska D, Krukowska-Bak J, Kazmierczak-Razna J, Pietrzak R (2017) Uptake of heavy metal ions from aqueous solutions by sorbents obtained from the spent ion exchange resins. *Micropor Mesopor Mater.* 244:127–136. <https://doi.org/10.1016/j.micromeso.2017.02.040>
- Kumar N, Sinha S, Mehrotra T, Singh R, Tandon S, Thakur I S (2019) Biodecolorization of azo dye acid black 24 by *Bacillus pseudomycolides*: process optimization using Box Behnken design model and toxicity assessment. *Bioresour Technol Rep.* 8 (100311): 1–11. <https://doi.org/10.1016/j.biteb.2019.100311>
- Kumar V, Giri BS, Raza N, Roy K, Kim Ki-Hyun, Rai B N, Singh RS (2018) Recent advancements in bioremediation of dye: current

- status and challenges. *Bioresour. Technol.* 253:355–367. <https://doi.org/10.1016/j.biortech.2018.01.029>
31. Kyi PP, Quansah JO, Lee CG, Moon JK, Park SJ (2020) The removal of crystal violet from textile wastewater using palm kernel shell derived biochar. *Appl Sci.* 10(7): 2251. <https://doi.org/10.3390/app10072251>
 32. Lagergren S (1898) About the theory of so-called adsorption of soluble substance. *Seven Vetenskapsakad HandBAnd* 24(4):1–39
 33. Lellis B, Fávoro-Polonio CZ, Pamphile JA, Polonio JC (2019) Effects of textile dyes on health and the environment and bioremediation potential of living organisms. *Biotechnol Res Inn* 3: 275–290. <https://doi.org/10.1016/j.biori.2019.09.001>
 34. Lonappan L, Rouissi T, Das RK, Brar SK, Ramirez AA, Verma M, Surampalli RY, Valero JR (2016) Adsorption of methylene blue on biochar microparticles derived from different waste materials. *Waste Manage* 49:537–544. <https://doi.org/10.1016/j.wasman.2016.01.015>
 35. Ma A, Abushaikha A, Allen SJ, McKay G (2019) Ion exchange homogeneous surface diffusion modelling by binary site resin for the removal of nickel ions from wastewater in fixed beds. *Chem Eng J.* 358: 1–10. <https://doi.org/10.1016/j.cej.2018.09.135>
 36. Mahmoodi NM (2013) Magnetic ferrite nanoparticle – alginate composite: synthesis, characterization and binary system dye removal. *J Taiwan Inst Chem Engineers.* 44:322–330. <https://doi.org/10.1016/j.jtice.2012.11.014>
 37. Mashkoo F, Nasar A, Inamuddin, Asiri AM (2018) Exploring the reusability of synthetically contaminated wastewater containing crystal violet dye using *Tectona grandis* sawdust as a very low-cost adsorbent. *Scientific Rep.* 8:8314. <https://doi.org/10.1038/s41598-018-26655-3>
 38. Namasivayam C, Prabha D, Kumutha M (1998) Removal of direct red and acid brilliant blue by adsorption on to banana pith. *Bioresour Technol.* 64:77–79. [https://doi.org/10.1016/S0960-8524\(97\)86722-3](https://doi.org/10.1016/S0960-8524(97)86722-3)
 39. Namasivayam C, Sumithra S (2005) Removal of direct red 12B and methylene blue from water by adsorption onto Fe (III)/Cr (III) hydroxide, an industrial solid waste. *J Environ Management* 74:207–215. <https://doi.org/10.1016/j.jenvman.2004.08.016>
 40. Namasivayam C, Yamuna RT (1995) Adsorption of direct red 12 B by biogas residual slurry: equilibrium and rate processes. *Environ Pollut* 89:1–7. [https://doi.org/10.1016/0269-7491\(94\)00056-J](https://doi.org/10.1016/0269-7491(94)00056-J)
 41. Ng C, Losso JN, Marshall WE, Rao RM (2002) Freundlich adsorption isotherms of agricultural by-product-based powdered activated carbons in a geosmin-water system. *Bioresour Technol* 85:131–135. [https://doi.org/10.1016/s0960-8524\(02\)00093-7](https://doi.org/10.1016/s0960-8524(02)00093-7)
 42. Ngulube T, Gumbo JR, Masindi V, Maity A (2017) An update on synthetic dyes adsorption onto clay based minerals: a state-of-art review. *J Environ Manage* 191:35–57. <https://doi.org/10.1016/j.jenvman.2016.12.031>
 43. Oguntimein G, Hunter J, Kang D (2014) Biosorption of azure dye with sunflower seed hull: estimation of equilibrium, thermodynamic and kinetic parameters. *Inter J Eng Res Dev* 10:26–41
 44. Ojha AK, Bulasara VK (2015) Adsorption characteristics of jackfruit leaf powder for the removal of Amido black 10B dye. *Environ Prog Sustainable Energy* 34(2):461–470. <https://doi.org/10.1002/ep.12015>
 45. Oladipo AA, Gazi M (2014) Enhanced removal of crystal violet by low cost alginate/acid activated bentonite composite beads: optimization and modelling using non-linear regression technique. *J Water Proc. Eng.* 2:43–52. <https://doi.org/10.1016/j.jwpe.2014.04.007>
 46. Pham TD, Bui TT, Nguyen VT (2018) Adsorption of polyelectrolyte onto nanosilica synthesized from rice husk: characteristics, mechanisms, and application for antibiotic removal. *Polymer.* 10 (2):2–17. <https://doi.org/10.3390/polym10020220>
 47. Regti A, Laamari MR, Stiriba SE, Haddad ME (2017) Removal of basic blue 41 dyes using *Persea americana*-activated carbon prepared by phosphoric acid action. *Int J Ind Chem.* 8:187–195. <https://doi.org/10.1007/s40090-016-0090-z>
 48. Roy K, Verma KM, Kumar V, Goswami M, Sonwani RK, Rai BN, Vellingiri K, Kim K H, Giri BS, Singh RS (2018) Removal of patent blue (V) dye using Indian bael shell biochar: characterization, application and kinetic studies. *Sustainability.* 10 (2669):1–13. <https://doi.org/10.3390/su10082669>
 49. Safa Y, Bhatti HN (2011) Adsorptive removal of direct dyes by low cost rice husk: effect of treatments and modifications. *African J Biotechnol* 10(16):3128–3142. <https://doi.org/10.5897/AJB10.1302>
 50. Sankar M, Sekaran G, Sadulla S, Ramasami T (1999) Removal of diazo and triphenylmethane dyes from aqueous solutions through an adsorption process. *J Chem Technol Biotechnol* 74:337–344. [https://doi.org/10.1002/\(SICI\)1097-4660\(199904\)74:4%3c337::AID-JCTB39%3e3.0.CO;2-U](https://doi.org/10.1002/(SICI)1097-4660(199904)74:4%3c337::AID-JCTB39%3e3.0.CO;2-U)
 51. Semmoud R, Didi MA (2019) An efficient cloud point extraction of mixed organic/inorganic pollutants using an ionic liquid as extractant: separation of the red Bemacid dye from nickel (II) in saline medium and optimization through factorial design methodology. *Desalin Water Treat* 152:393–400. <https://doi.org/10.5004/dwt.2019.23900>
 52. Soltani RDC, Khataee A, Koolivand A (2015) Kinetic, isotherm, and thermodynamic studies for removal of direct red 12B using nanostructured biosilica incorporated into calcium alginate matrix. *Environ Progress and Sustainable Energy* 34(5):1435–1443. <https://doi.org/10.1002/ep.12146>
 53. Tripathi R, Gupta A, Thakur IS (2019) An integrated approach for phycoremediation of wastewater and sustainable biodiesel production by green microalgae, *Scenedesmus* sp. ISTGA1. *Renew Energy* 135:617–625. <https://doi.org/10.1016/j.renene.2018.12.056>
 54. Varjani S, Rakholiya P, Yong Ng H, You S, Teixeira JA (2020) Microbial degradation of dyes: an overview. *Bioresour Technol* 314:123728. <https://doi.org/10.1016/j.biortech.2020.123728>
 55. Vyavahare GD, Gurav RG, Jadhav PP, Patil RR, Aware CB, Jadhav JP (2018) Response surface methodology optimization for sorption of malachite green dye on sugarcane bagasse biochar and evaluating the residue dye for phyto and cytogenotoxicity. *Chemosphere* 194:306–315. <https://doi.org/10.1016/j.chemosphere.2017.11.180>
 56. Wang HC, Cui D, Yang LH, Ding YC, Cheng HY, Wang AJ (2017) Increasing the bio-electrochemical system performance in azo dye wastewater treatment: reduced electrode spacing for improved hydrodynamics. *Bioresour Technol.* 245(Part A):962–969. <https://doi.org/10.1016/j.biortech.2017.09.036>
 57. Wang Y, Zhang C, Zhao L, Meng G, Wu J, Liu Z (2017) Cellulose-based porous adsorbents with high capacity for methylene blue adsorption from aqueous solutions. *Fibers Polymers* 18:891–899. <https://doi.org/10.1007/s12221-017-6956-7>
 58. Zazyckia MA, Godinhob M, Perondib D, Folettoa EL, Collazzoa GC, Dotto GL (2018) New biochar from pecan nutshells as an alternative adsorbent for removing reactive red 141 from aqueous solutions. *J Clean Prod* 171:57–65
 59. Zhou MY, Zhang P, Fang LF, Zhu BK, Wang JL, Chen JH, Abdallah HM (2019) A positively charged tight UF membrane and its properties for removing trace metal cations via electrostatic repulsion mechanism. *J Hazard Mater* 373:168–175. <https://doi.org/10.1016/j.jhazmat.2019.03.088>

Publisher's note Springer Nature remains neutral with regard to jurisdictional claims in published maps and institutional affiliations.